Interplay between oxygen vacancies and cation ordering in the NiFe_2O_4 spinel ferrite

Rémi Arras, Kedar Sharma, Lionel Calmels

Journal Name

ARTICLE TYPE

Cite this: DOI: 00.0000/xxxxxxxxxx

Interplay between oxygen vacancies and cation ordering in the $NiFe_2O_4$ spinel ferrite†

Rémi Arras,*[a] Kedar Sharma,[a] and Lionel Calmels[a]

Received Date
Accepted Date

DOI: 00.0000/xxxxxxxxxx

The spinel ferrite $NiFe_2O_4$ is a ferrimagnetic material with a high Curie temperature, highly promising for spintronic applications. Its magnetic and electronic properties strongly depend on the presence of structural defects, in particular the cation disorder (described by the inversion degree) and oxygen vacancies, which are very common in oxides. We performed first-principle calculations to study the interplay between these two kinds of defects, which have up-to-now mostly been considered independently, while they do coexist in real samples. We show that the complex formed by a Ni_{Oh}/Fe_{Td}-cation swap and a neutral oxygen vacancy is more stable than these two isolated defects. Such complexes strongly reduce the width of the minority-spin band gap due to the creation of gap states. We propose an equation, potentially useful to analyze experimental data, which describes the dependence of the magnetization on the inversion degree and on the oxygen-vacancy content.

1 Introduction

Spinel ferrites are attractive for a large variety of applications, in particular in the fields of catalysis[1–4], electronics and spintronics[5,6]. A noticeable interest in ferrites comes from their chemical composition which includes two very abundant and non-toxic elements, i.e. iron and oxygen. To improve the performances of ferrite-based devices, a good control of their electronic and magnetic properties is mandatory, which can only be reached with a good understanding of the intricate coupling between their atomic structure and these properties.

$NiFe_2O_4$ (NFO) is an interesting member of the ferrite family because of its insulating character and ferrimagnetic ordering with a high Curie temperature of ∼858 K[7]. This oxide is expected to possess a structure close from the inverse spinel one, which can be described by the chemical formula $(Fe^{3+})_{Td}[Ni^{2+},Fe^{3+}]_{Oh}(O^{2-})_4$. The term *inverse* refers to the position of the divalent cations Ni^{2+} which are only located in the octahedral (Oh) sites, instead of the tetrahedral (Td) sites, which they would occupy if the spinel structure was *normal*. The inversion degree λ is a parameter with a value varying between 0 and 1, which characterizes the amount of divalent cations distributed between the two crystallographic sites, according to $(Ni^{2+}_{1-\lambda}Fe^{3+}_{\lambda})_{Td}[Ni^{2+}_{\lambda}Fe^{3+}_{2-\lambda}]_{Oh}(O^{2-})_4$; $\lambda = 1$ thus corresponds to the fully-inverse spinel structure. The cation distribution is the first structural parameter which can drastically influence the electronic properties of a spinel oxide[8–10]. Even if so-called inverse spinel ferrites are mostly found with an inversion degree lower than 1, it has been shown that NFO can be grown with a perfectly inverse structure and an ordering of the Fe/Ni cations inside the Oh sublattice corresponding to the space group $P4_122$ (No. 91)[11,12]. The cation distribution remains nonetheless dependent on the growth conditions, thermal post-treatments, the choice of the substrate and the sample dimension and size[13,14]. A lowering of the inversion parameter is expected to have for consequences a decrease of the band gap as well as an increase of the magnetization as Fe^{3+} cations possess a higher spin magnetic moment ($\sim 5\ \mu_B$ in the isolated-ion limit) than the Ni^{2+} ($\sim 2\ \mu_B$)[10,13].

Electronic and magnetic properties are also likely to be modified by the presence of point defects such as atom vacancies. In a recent study[10], we showed that charged Ni vacancies and neutral O vacancies (V_O^0) are the most probable of these defects, under an oxygen-rich or oxygen-poor growth condition, respectively. Oxygen vacancies are a common type of defects in oxides. They play an important role for the development of future non-volatile memory devices based on resistive-switching processes[15–17]. In spinel ferrites, they have already been mentioned in experimental studies as the hypothetical cause for the modification of the tunnel conductivity through vacancy gap states[18], or for the decrease of the magnetization due to the decrease of the oxidation degree of the Fe_{Oh} and Ni_{Oh} cations[19]. However, in our previous numerical studies[10,20], we used *ab initio* calculations to show that neutral oxygen vacancies indeed induce electronic gap states, but are not likely to change the magnetization.

In already-published numerical studies, several kinds of point defects have been considered separately[8,10,20,21]. Few experi-

[a] CEMES, Université de Toulouse, CNRS, 29 rue Jeanne Marvig, F-31055, Toulouse, France E-mail: remi.arras@cemes.fr

† Electronic Supplementary Information (ESI) available: Details about the calculations of formation energies, detailed results on every studied structure, dependency on the U_{eff} parameter and variations of the atomic spin magnetic moments. See DOI: 00.0000/00000000.

mental works however pointed out that a correlation exist between the cation disorder and the presence of oxygen vacancies[22–26], which was confirmed numerically in the normal spinel $ZnFe_2O_4$[27]. In this paper, we analyze the possible coupling between the formation of oxygen vacancies and the inversion degree when it slightly deviates from 1. We show that the formation of oxygen vacancies is more probable near the Ni cations located in Td sites which would result from Fe_{Td}/Ni_{Oh} swaps. We demonstrate that the oxygen vacancies only decrease the spin magnetization when such scenario occurs, because of the apperance of additional occupied states in the minority-spin band gap only, which should additionnally have an effect on the transport properties.

2 Details of calculations

We performed *ab initio* calculations based on the density functional theory (DFT). We have used the VASP code[28,29] with the projector augmented wave (PAW) method[30] and a cut-off energy of 600 eV. The exchange-correlation energy was calculated thanks to the functional proposed by Perdew, Burke, and Ernzerhof and revised for solids (GGA-PBESol)[31]. A Hubbard correction was added, in the framework of the DFT+U formalism[32], in order to take the strong correlations of the transition metal 3d bands into account. We used the same $U_{\text{eff}} = (U - J)$ parameters as in our previous study[10], i.e. 4.0 eV for Fe and 2.5 eV for Ni atoms. To calculate the effects of a neutral oxygen vacancy, we used a supercell approach with a $1 \times 1 \times 1$ conventional cubic cell of 8 formula units (f.u.) which possesses 56 atoms. Every structure has been optimized by minimizing the forces down to less than 0.01 eV Å^{-1} and calculating equilibrium lattice parameters with a convergence criterium on the total energy of 0.001 eV/f.u. A Monkhorst-Pack grid[33] of $6 \times 6 \times 6$ $\boldsymbol{k}$-vectors was used to sample the first Brillouin zone.

The formation energy of the neutral oxygen vacancies $E_f[V_O^0]$ is calculated following the same methodology as in Ref.[10] and according to the theory described in Ref.[34]. It depends on the chemical potential of the oxygen atoms, that we fixed to $\mu_O = 0.5E_{O_2} + \Delta\mu_O = -6.432$ eV, where E_{O_2} is the calculated total energy of an O_2 molecule and $\Delta\mu_O$ is obtained from a thermodynamic model[10,35], considering a growth temperature $T = 673$ K and an oxygen pressure $P = 1.3 \times 10^{-6}$ mbar[23]. We remind that the variations of the formation energy, for a given concentration of vacancies, only depend on variations of the total energy of the defective cell and are independent on the value of the oxygen chemical potential which is kept constant. More information about the dependency of our results on the choice of the U_{eff} values, the stability of the magnetic ordering and on the thermodynamic models are given in the ESI†.

3 Results

When NFO is stoichiometric and crystallizes in its inverse-spinel structure ($\lambda = 1$), the most homogeneous distribution of Ni^{2+} and Fe^{3+} cations in Oh sites corresponds to the space group $P4_122$, which is the structure with the lowest energy[8,10–12] [see Fig. 1(a)]. With this cation distribution, the lattice is slightly tetragonal, with lattice parameters of $a = b = 8.279$ Å and $c = 8.295$ Å, which corresponds to an equilibrium pseudo-cubic parameter of $a_{pc} = 8.284$ Å, in agreement with the experimental value of 8.339 Å[36]. In this structure, each oxygen atom has one Td and three Oh occupied cation sites as first neighbors. With the cation distribution associated to the $P4_122$ space group, we can distinguish two non-equivalent sets of oxygen atoms: half of them have two Fe_{Oh} and one Ni_{Oh} as first neighbors, the others have one Fe_{Oh} and two Ni_{Oh} first neighbors. All oxygen atoms have one Fe_{Td} atom as first neighbor when $\lambda = 1$. If we characterize an oxygen atomic site by its number of Fe first neighbors in Td and Oh sites (n_{Td}, n_{Oh}), the two kinds of oxygen atoms are thus labeled $(1,1)$ and $(1,2)$ [Fig. 1(b)]. This perfect structure will be considered as the reference in the following and defects will be created in this cell.

Making the approximation that the spin magnetic moment of each cation in the crystal is close to that of an isolated ion, we can attribute the spin magnetic moments of 2 μ_B and 5 μ_B to Ni^{2+} and Fe^{3+} cations respectively. Because of the ferrimagnetic ordering, defined by the antiferromagnetic coupling betwen cations in Oh and Td sites and the ferromagnetic ordering between cations in Oh sites[9,10,37], we expect a total spin magnetic moment of 2 μ_B/f.u. of NFO, as confirmed by our DFT calculations. The density of states (DOS) [Fig. 2(a)] shows that NFO is insulating, with majority- and minority-spin band gaps of 1.92 eV and

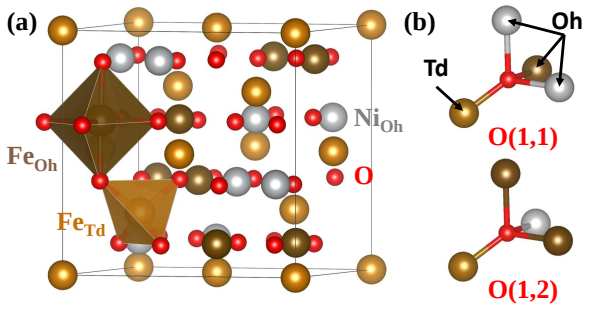

Fig. 1 (a) $1 \times 1 \times 1$ conventional cubic cell of the $NiFe_2O_4$ inverse spinel structure. The Fe_{Oh}/Ni_{Oh} cation distribution corresponds to the $P4_122$ space group. (b) First-neighbor chemical environment of the two non-equivalent oxygen atoms $O(n_{Td}, n_{Oh})$ of the $P4_122$ space group.

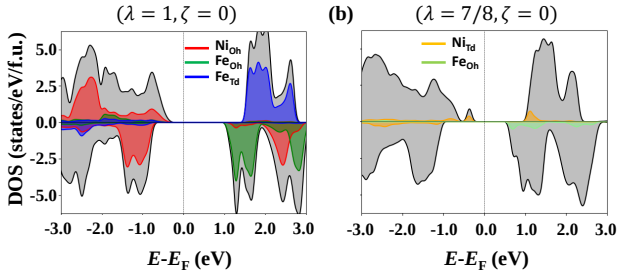

Fig. 2 Total and projected density of states (DOS) calculated for (a) the perfect inverse spinel NFO structure and (b) the structure with a Fe_{Td}/Ni_{Oh} exchange ($\lambda = 0.875$). The total DOS is given in gray and the atomic projections in colors: for the perfect structure (a), they correspond to the contribution of all atoms of a specific kind, while in the subfigure (b), only the contributions of exchanged atoms (orange and light green) are shown. Positive and negative DOS values correspond to majority- and minority-spin states.

1.887 eV respectively. The overall band gap of 1.42 eV is delimited by the majority-spin valence band maximum (VBM) with a Ni_{Oh}-3d + O-2p character and the minority-spin conduction band minimum (CBM), mostly with a Fe_{Oh}-3d character.

3.1 Cation inversion between Td and Oh sites

We will now remind how the properties change when the structure is stoichiometric but not fully inverse. We considered a supercell in which we swapped one Ni^{2+}_{Oh} with one Fe^{3+}_{Td} cation, which corresponds to the inversion degree $\lambda = 0.875$. We identified several different ways of swapping these ions: Firstly, the swap can occur between first-neighbor cations bonded to a common O(1,1) or O(1,2) atom. These swaps will be labeled $S_1(1,1)$ and $S_1(1,2)$, respectively. The last configurations (S_2) are obtained by swapping more distant neighbors (second neighbors, considering the dimension of our supercell). The structures with $\lambda = 0.875$ are all less stable than that with $\lambda = 1$. The more stable of the newly created structures corresponds to the swap $S_1(1,1)$, with $\Delta E = E[\lambda = 0.875, S_1(1,1)] - E[\lambda = 1] = 1.066$ eV. Other structures are less stable by 7 meV [$S_1(1,2)$] and 92 meV (S_2). First-neighbor exchanges are thus easier to form and give rise to structures with nearly the same energy.

Due to the ferrimagnetic ordering, the total spin magnetic moment M (per f.u.) is expected to vary as a function of the inversion degree[10] as:

$$M(\lambda) = (-6\lambda + 8)\mu_B \quad (1)$$

which leads to a spin magnetic moment of 2.75 μ_B/f.u. for $\lambda = 0.875$ (i.e. an increase by 0.75 μ_B with respect to the crystal with $\lambda = 1$), as confirmed by our DFT calculations. Fig. 2(b) shows that the presence of a Ni atom in a Td site induces the appearance of a gap state just above the bulk VBM in the majority-spin channel. The rest of the d bands of this Ni atom are unoccupied and located at the CBM.

3.2 Oxygen vacancies in the perfectly inverse spinel structure

Let us now describe the electronic properties in the presence of a neutral oxygen vacancy V^0_O in the perfectly inverse spinel crystal. The new chemical composition is $NiFe_2O_{4-\zeta}$, where $\zeta = 0.125$ corresponds to a content of oxygen vacancies of 3.125%. When $\lambda = 1$, oxygen vacancies can form by removing one of the two kinds of oxygen atoms. As reported in Table 1, the formation energy of a neutral vacancy $V^0_O(1,1)$ is 99 meV lower than that of a $V^0_O(1,2)$.

As reported in our previous studies, a neutral oxygen vacancy does not change the total spin magnetic moment of an inverse spinel ferrite[10,20]. This phenomenon can be explained by the facts that (1) among the two electrons which are released by the vacancy to preserve the electric neutrality, one is equally distributed on the cations in the Oh sites first neighbors of the vacancy, while the other one will be located on the Fe cation in the nearest Td site, and (2) the ferrimagnetic ordering in spinel ferrites is governed by the strong antiferromagnetic couplings between the cations in Td and Oh sites and it is preserved for the low content of V^0_O that we considered. As it can be seen in the

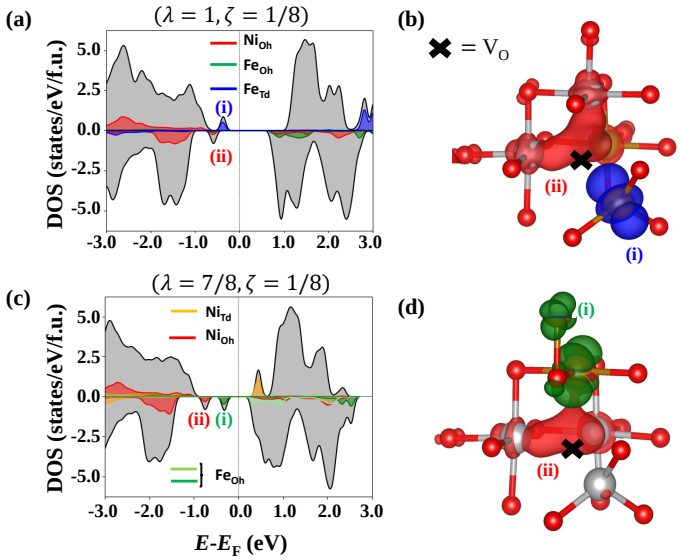

Fig. 3 Total (gray area) and projected density of states (DOS) and charge densities calculated for (a,b) the inverse spinel structure possessing an oxygen vacancy in the (1,1) site (see Table 1) and (c,d) the most stable structure with a complex defect formed by the association of a cation swap and an oxygen vacancy in a (0,1) atomic site. In subfigures (a,c), the DOS projected onto atomic sites are given in colors; only the contributions of the atoms first-neighbors of the oxygen vacancy (red, orange, blue, dark green) and the exchanged atoms (orange and light green) are shown. Positive and negative DOS values correspond to majority- and minority-spin states. The density of charges in subfigures (b,d) correspond to the gap states labeled in subfigures (a,c).

DOS curves of Fig. 3(a), one of the electrons released by the V^0_O occupies the Fe^{3+}_{Td}-d_{z^2} band, which corresponds to the gap state (i) near the VBM in the majority-spin channel; this first transferred electron decreases (increases) the spin magnetic moment of this cation (of NFO) by ~ 0.44 μ_B. The second transferred electron occupies the minority-spin defect state (ii), formed from the hybridization of Fe_{Oh}- and Ni_{Oh}-3d with O-2p orbitals. We can indeed see that the charge density associated to this defect state, plotted in Fig. 3(b), is largely delocalized onto the three Oh cations first neighbors of the vacancy, and even onto some of the surrounding oxygen atoms. Such a result is consistent with the reduction of Ni cations, as reported by Anjum, *et al.*[19]. This second electron transfer decreases the spin magnetic moment of each of the three first-neighbor cations in Oh sites by approximately 0.13 μ_B each (see Table II in the ESI†). These values explain why the total spin magnetic moment calculated for the oxygen-deficient NFO crystal remains of 2.0 μ_B/f.u., the same as for the stoichiometric structure.

We now discuss how the oxygen vacancies and Fe_{Td}/Ni_{Oh} cation swaps interact together.

3.3 Formation of a complex defects formed by the combination of an oxygen vacancy and a cation inversion

We first analyze the formation of oxygen vacancies when the spinel structure is not fully-inverse. Owing to the structural distortions and to the cation distribution, all the 32 oxygen atoms of the supercell are non equivalent when $\lambda = 0.875$. We calculated

Table 1 Total spin magnetic moment M_S per f.u. of NFO and averaged formation energy E_f of a neutral oxygen vacancy and pseudo-cubic lattice parameter a_{pc}, calculated with different inversion degrees λ and at different oxygen sites, described by $[n_{Td}(Fe), n_{Oh}(Fe)]$ (the multiplicity n_i of these sites in the cubic supercell is also given for information).

λ		M_S (μ_B/f.u.)	$[n_{Td}(Fe), n_{Oh}(Fe)]$	n_i	$E_f(V_O^0)$ (eV)	a_{pc} Å
1		2.0	(1,1)	16	2.756	8.286
			(1,2)	16	2.855	8.291
		multiplicity-weighted average			2.806	8.288
0.875	$S_1(1,1)$	2.5	(0,1)	1	2.190	8.284
			(0,2)	3	2.284	8.284
		2.75	(1,1)	11	2.722	8.296
			(1,2)	15	2.844	8.300
			(1,3)	2	2.939	8.304
		multiplicity-weighted average			2.735	8.297

the formation energies of an oxygen vacancy by considering the 32 possible locations of this vacancy in the non-inverse structure with a $S_1(1,1)$ swap (as shown in the ESI†, the calculated values are nearly independent of the choice of the Fe_{Td} and Ni_{Oh} swapped atoms). In Table 1, we report the formation energies, averaged over all the possible vacancy locations with similar first-neighbor chemical environement. The averaged formation energy varies as a function of the numbers of Fe atoms (n_{Td} and n_{Oh}) first neighbors of the vacancy: it increases by approximately 0.1 eV [0.5 eV] when n_{Oh}(Fe) [n_{Td}(Fe)] increases by 1. At $T = 0$ K, oxygen vacancies are expected to form preferentially at the atomic sites which correspond to the lowest formation energy. Oxygen vacancies are thus more likely to form where the cation distribution is locally normal (*i.e.* Ni^{2+} cations occupy Td sites), in particular if the site is also poor in Fe_{Oh} atoms.

Conversely, we now try to understand how an oxygen vacancy can disturb the cation ordering and locally modify the inversion degree λ. From the previous discussion, we can assume that an oxygen vacancy will primarily form in the (1,1) atomic sites of a perfectly inverse spinel structure ($\lambda = 1$). The environment near this oxygen vacancy can become poorer in Fe atoms when λ decreases, with the formation of (0,1) sites: in the presence of an oxygen vacancy, swapping one Fe_{Td}^{3+} with one Ni_{Oh}^{2+} cation costs an energy of $\Delta E = E[\lambda = 0.875, V_{O(0,1)}] - E[\lambda = 1, V_{O(1,1)}] = 0.500$, 0.515 and 0.588 eV, for $S_1(1,1)$, $S_2(1,2)$ and S_2 respectively. These energies are twice smaller than those reported above for stoichiometric NFO ($\simeq 1$ eV). This confirms the intimate link between the oxygen stoichiometry and the inversion degree. From this result, we can infer that the formation of oxygen vacancies during a growth in oxygen-poor environment facilitates the formation of non-inverse spinel structures.

Finally, to estimate the stability of the complex formed by a cation swap and an oxygen vacancy, we have calculated the binding energy[34] E_b which corresponds to the difference between the formation energy of the complex $E_f[\lambda = 0.875, \zeta = 0.125]$ calculated with respects to the energy of the ground-state stoichiometric structure ($\lambda = 1$ and $\zeta = 0$) and the sum of the formation energies of each defect considered separately. We found that $E_b = -0.566$ eV. This negative value confirms the stability of the complex and the tendency of the two defects to bond together.

3.4 Effect induced by the oxygen-vacancy/cation-inversion complex on the physical properties

The first effect of the formation of the complex formed by the association of an oxygen vacancy and a Ni/Fe inversion consists in a slight increase of the pseudo-cubic lattice parameter a_{pc} if compared with the stoichiometric and inverse structure. As displayed in Table 1, the presence of an oxygen vacancy induces an averaged increase of this parameter by only 0.04%, while the increase is of 0.16% in the presence of the complex. It is important that owing the particular cation distribution and the presence of the oxygen vacancy, the system does not possess any local symmetry and most of the calculated configurations with the defect complex possess a triclinic structure, even if the deviation from the cubic structure are small. For example, for the structure with the lowest formation energy, we calculated that the in-plane lattice parameters a and b differs only by 0.4%, while the ration between the out-of-plane and in-plane parameters is of 1.003, close from the value of 1.002 calculated for the non-defective structure.

Regarding the magnetic and electronic properties, we first confirmed that the ferrimagnetic state of the perfect $NiFe_2O_4$ structure remains unchanged when the defects are present. More details about all the magnetic orderings which have been tested are given in the Table III of the ESI†. As explained before, a neutral oxygen vacancy does not change the spin magnetization of a fully inverse spinel structure. The situation is different for a vacancy in a not-fully-inverse spinel structure. In this case, the calculated spin magnetic moment depends on the location of the oxygen vacancy, more precisely on the chemical nature of the first-neighbor Td cation. When the inversion degree is $\lambda = 0.875$ and the first-neighbor Td site is occupied by an Fe cation, *i.e.* when the structure is locally inverse ($n_{Td} = 1$), the total spin magnetic moment of the NFO crystal does not change and remains of 2.75 μ_B/f.u., the same as for the stoichiometric compound with the same inversion degree. Conversely, if the local chemical environement is normal ($n_{Td} = 0$), the two released electrons localize onto cations in the first-neighbor Oh sites, as it can be seen in Fig. 3(c) and (d): the two gap states (i) and (ii) are now in the minority-spin channel, while Ni_{Td}-d orbitals form an unoccupied DOS peak near the majority-spin CBM. The two occupied gap states almost completely destroy the minority-spin band gap, which could induce a possible change of charge conductivity in the presence of oxygen vacancies. The V_O^0 state (ii) (with the lowest energy) is of the same nature in the partially-inverse spinel structure than in the fully-inverse one; the state (i) mainly involves the Fe_{Oh} first neighbor of the vacancy. These occupied gap states induce a reduction of the spin magnetic moment of the two first-neighbor Ni_{Oh} cations by 0.17 μ_B and of the Fe_{Oh} cation by 0.49 μ_B, hence decreasing the total spin magnetic moment of NFO by $\Delta m = 2.0$ μ_B/V_O^0. With a density of oxygen vacancies of 0.125 f.u.$^{-1}$, the total magnetic moment is thus decreased to 2.5 μ_B/f.u. (i.e. by 0.25 μ_B). Oxygen vacancies in NFO with a non-inverse spinel structure should preferentially correspond to oxygen atoms removed near Ni_{Td} atoms, when these atoms exist. The corresponding decrease of the magnetization thus occurs until all the existing Ni_{Td} have been involved in the formation of

a cation swap/oxygen vacancy complex. The total spin magnetic moment per f.u. can thus be described by:

$$M(\lambda,\zeta) = (-6\lambda + 8)\mu_B - n\Delta m \quad (2)$$

with $\Delta m = 2.0\ \mu_B$ and $n \leq (1-\lambda)$ is the number of oxygen vacancies first neighbors of a Ni_{Td} atom; if $\zeta \leq (1-\lambda)$, then $n = \zeta$, while if $\zeta > (1-\lambda)$, $n = (1-\lambda)$ and the $(\zeta - n)$ remaining vacancies are located near a Fe_{Td} atom.

This equation depends on different approximations. Firstly, we only studied the formation of a complex associating a Ni_{Td} and only one neutral oxygen vacancy; in addition, we considered an homogeneous distribution of these defects. If several oxygen vacancies were likely to form near the same Ni_{Td} atom, it would be necessary to study other complexes by using larger supercells, which is beyond the scope of this work. Secondly, this equation is mostly valid at low growth temperature, when oxygen vacancies are expected to form preferentially in atomic sites with the lowest formation energies. Conversely, at high temperature, the occurence of oxygen vacancy located in sites with higher formation energies would increase. If the oxygen vacancy would equally be located at all the different kinds of oxygen atomic sites, the total spin magnetic moment would then be given by:

$$M(\lambda) = (-6\lambda + 8)\mu_B - \Delta m(1-\lambda)\zeta \quad (3)$$

The variation of total spin magnetic moment as a function of the temperature is thus expected to be complex, the inversion degree λ and the content of oxygen vacancies ζ both depending on the temperature.

In their experimental investigation performed on polycrystalline thin films of $NiFe_2O_4$, Jaffari, *et al.*[23] measured the simultaneous presence of cation disorder and oxygen vacancies. While the lowering of the inversion degree should induce an increase of the magnetization, they measured instead that it decreased. They explained this measurement by the formation of a spin-glass state resulting from the lower number of superexchange Td-O-Oh antiferromagnetic coupling, which is due to the presence of the oxygen vacancies. Because of the strength of this Td-O-Oh coupling, we expect the ferrimagnetic ordering to be robust, which suggests a high content of oxygen vacancies in their samples. The authors of this paper indeed estimated that the inversion degree of their sample was of $\lambda = 0.69$ and they measured that 24% of the Fe cations had a 2+ oxidation state, and 13% of the Ni cations an oxidation state of 0. We thus expect that our study will motivate new investigations, in particular to verify to which extent our results could be generalized to other spinel ferrites, NFO being a particular member in the spinel-ferrite family, as Ni^{2+} cations possess a high Oh-site selectivity; stronger effects and correlations could be encounter in other spinel compounds. The role of oxygen vacancies is notably important as it can favor cation diffusions and make the cationic redistribution easier. The combined control of cation ordering and oxygen stoichiometry, as we demonstrated, is thus essential to tune in a predictive way the electronic and magnetic properties in view of optimizing future devices in the domains of catalysis and electronics. As shown by our calculations, the simultaneous presence of a sufficient amount of oxygen vacancies and cation exchanges between Td and Oh sites results could turn the Ni spinel ferrite into a metal with a high spin polarization of the DOS at the Fermi level, which could be interesting for spintronic devices. Studying the effects of these defects on the transport properties thus appears as an interesting perspective to this work[38].

Author Contributions

R. Arras: Conceptualization, Formal Analysis, Funding Acquisition, Investigation, Methodology, Resources, Writing - Original Draft, Writing - Review & Editing, K. Sharma: Review & Editing, L. Calmels: Formal Analysis, Review & Editing

Conflicts of interest

There are no conflicts to declare.

Acknowledgements

This study has been supported through the ANR Grant ANR-19-CE09-0036. This work was granted access to the HPC resources of CALMIP (Allocation No. 2023/P1229).

Notes and references

1 X. Shi, Y.-F. Li, S. L. Bernasek and A. Selloni, *Surf. Sci.*, 2015, **640**, 73.
2 H. Hajiyani and R. Pentcheva, *ACS Catal.*, 2018, **8**, 11773–11782.
3 H. Zhong, G. Gao, X. Wang, H. Wu, S. Shen, W. Zuo, G. Cai, G. Wei, Y. Shi, D. Fu, C. Jiang, L.-W. Wang and F. Ren, *Small*, 2021, **17**, 2103501.
4 Y. Peng, C. Huang, J. Huang, M. Feng, X. Qiu, X. Yue and S. Huang, *Adv. Funct. Mater.*, 2022, **32**, 2201011.
5 R. Valenzuela, *Phys. Res. Int.*, 2012, **2012**, 591839.
6 A. Hirohata, H. Sukegawa, H. Yanagihara, I. Žutić, T. Seki, S. Mizukami and R. Swaminathan, *IEEE Trans. Magn.*, 2015, **51**, 1.
7 S. Ziemniak, L. Anovitz, R. Castelli and W. Porter, *J. Phys. Chem. Solids*, 2007, **68**, 10.
8 D. Fritsch and C. Ederer, *Appl. Phys. Lett.*, 2011, **99**, 081916.
9 K. R. Sanchez-Lievanos, J. L. Stair and K. E. Knowles, *Inorg. Chem.*, 2021, **60**, 4291.
10 K. Sharma, L. Calmels, D. Li, A. Barbier and R. Arras, *Phys. Rev. Mater.*, 2022, **6**, 124402.
11 V. G. Ivanov, M. V. Abrashev, M. N. Iliev, M. M. Gospodinov, J. Meen and M. I. Aroyo, *Phys. Rev. B*, 2010, **82**, 024104.
12 J. K. Dey, A. Chatterjee, S. Majumdar, A.-C. Dippel, O. Gutowski, M. v. Zimmermann and S. Giri, *Phys. Rev. B*, 2019, **99**, 144412.
13 U. Lüders, M. Bibes, J.-F. Bobo, M. Cantoni, R. Bertacco and J. Fontcuberta, *Phys. Rev. B*, 2005, **71**, 134419.
14 M. N. Iliev, D. Mazumdar, J. X. Ma, A. Gupta, F. Rigato and J. Fontcuberta, *Phys. Rev. B*, 2011, **83**, 014108.
15 W. Hu, N. Qin, G. Wu, Y. Lin, S. Li and D. Bao, *J. Am. Chem. Soc.*, 2012, **134**, 14658.
16 S.-K. Tong, J.-H. Chang, Y.-H. Hao, M.-R. Wu, D.-H. Wei and Y.-L. Chueh, *Appl. Surf. Sci.*, 2021, **564**, 150091.

17 J. Li, C. Yao, W. Huang, N. Qin and D. Bao, *J. Alloys Compd.*, 2022, **890**, 161814.
18 A. V. Ramos, T. S. Santos, G. X. Miao, M.-J. Guittet, J.-B. Moussy and J. S. Moodera, *Phys. Rev. B*, 2008, **78**, 180402.
19 S. Anjum, G. H. Jaffari, A. K. Rumaiz, M. S. Rafique and S. I. Shah, *J. Phys. D: Appl. Phys.*, 2010, **43**, 265001.
20 R. Arras, L. Calmels and B. Warot-Fonrose, *Appl. Phys. Lett.*, 2012, **100**, 032403.
21 K. Dileep, B. Loukya, N. Pachauri, A. Gupta and R. Datta, *J. Appl. Phys.*, 2014, **116**, 103505.
22 S. Ayyappan, S. P. Raja, C. Venkateswaran, J. Philip and B. Raj, *Appl. Phys. Lett.*, 2010, **96**, 143106.
23 G. H. Jaffari, A. K. Rumaiz, J. C. Woicik and S. I. Shah, *J. Appl. Phys.*, 2012, **111**, 093906.
24 X. Chen, X. Zhu, W. Xiao, G. Liu, Y. P. Feng, J. Ding and R.-W. Li, *ACS Nano*, 2015, **9**, 4210.
25 Y. Li, Y. Li, X. Xu, C. Ding, N. Chen, H. Ding and A. Lu, *Chem. Geol.*, 2019, **504**, 276.
26 Y. He, L. Zhang, H.-W. Xiong and X. Kang, *J. Alloys Compd.*, 2022, **917**, 165494.
27 J. Melo Quintero, K. Salcedo Rodríguez, C. Rodríguez Torres and L. Errico, *J. Alloys Compd.*, 2019, **775**, 1117–1128.
28 G. Kresse and J. Hafner, *Phys. Rev. B*, 1994, **49**, 14251.
29 G. Kresse and J. Furthmüller, *Phys. Rev. B*, 1996, **54**, 11169.
30 P. E. Blöchl, *Phys. Rev. B*, 1994, **50**, 17953.
31 J. P. Perdew, A. Ruzsinszky, G. I. Csonka, O. A. Vydrov, G. E. Scuseria, L. A. Constantin, X. Zhou and K. Burke, *Phys. Rev. Lett.*, 2008, **100**, 136406.
32 S. L. Dudarev, G. A. Botton, S. Y. Savrasov, C. J. Humphreys and A. P. Sutton, *Phys. Rev. B*, 1998, **57**, 1505.
33 H. J. Monkhorst and J. D. Pack, *Phys. Rev. B*, 1976, **13**, 5188.
34 C. Freysoldt, B. Grabowski, T. Hickel, J. Neugebauer, G. Kresse, A. Janotti and C. G. Van de Walle, *Rev. Mod. Phys.*, 2014, **86**, 253.
35 J. Osorio-Guillén, S. Lany, S. V. Barabash and A. Zunger, *Phys. Rev. Lett.*, 2006, **96**, 107203.
36 R. C. Liebermann, *Phys. Earth Planet. Inter.*, 1972, **6**, 360.
37 M. C. Richter, J. M. Mariot, O. Heckmann, L. Kjeldgaard, B. S. Mun, C. S. Fadley, U. Lüders, J.-F. Bobo, P. De Padova, A. Taleb-Ibrahimi and K. Hricovini, *Eur. Phys. J. Special Topics*, 2009, **169**, 175.
38 M. H. N. Assadi, J. J. Gutiérrez Moreno and M. Fronzi, *ACS Appl. Energy Mater.*, 2020, **3**, 5666–5674.